

Taguchi optimization of photodegradation of yellow water of trinitrotoluene production catalyzed by nanoparticles TiO_2/N under visible light

Hamid Reza Pouredal*, Mohammad Fallahgar, Fahimeh Sotoudeh Pourhasan, Mohammad Nasiri

Faculty of Applied Chemistry, Malek-ashtar University of Technology, Shahin-Shahr, I. R. Iran.

Received 7 June 2017; received in revised form 23 July 2017; accepted 14 August 2017

ABSTRACT

Taguchi experimental design technique was used for optimization of photodegradation of yellow water sample of trinitrotoluene (TNT) production process. The nanoparticles of doped N- TiO_2 were also used as photocatalysts in the photodegradation reaction under visible light. The ranking of data based on signal to noise ratio values showed that the importance order of the factors affecting the degradation efficiency was: the nature of photocatalyst > time of photodegradation > amount of photocatalyst > initial concentration of pollutant. The optimized conditions were photocatalyst of $\text{TiO}_2/\text{N}_{0.1}$ photocatalyst dosage of 1.5 g L^{-1} and dilution times of 750 for real samples. The photocatalyst of $\text{TiO}_2/\text{N}_{0.1}$ was analyzed by BET surface analysis, X-ray diffraction pattern, field emission scanning electron microscopy (FE-SEM), energy-dispersive X-ray spectroscopy (EDS) and diffuse reflectance spectra (DTS). Relatively high surface area of $150 \text{ m}^2 \cdot \text{g}^{-1}$, anatase/rutile structure, approximately uniform distribution of nanoparticles size and band-gap energy of 2.92 eV were measured for $\text{TiO}_2/\text{N}_{0.1}$ nanophotocatalyst. A linear model with the regression coefficient (R^2) of 0.887 was obtained by the multiple linear regression analysis. The proposed model was "Degradation efficiency (Y) = $20.492 + 1.461 X_1 + 6.330 X_2 + 0.014 X_3 + 2.291 X_4$ ". The obtained P-values in the confidence level of 95% were < 0.05, showing a meaningful addition in the model. Therefore, changes in the predictor's value are due to changes in the response variable.

Keywords: Taguchi method, Doped TiO_2 nanophotocatalyst, Yellow water, Photodegradation.

1. Introduction

Taguchi method was used as a statistical method for optimization of experimental design [1]. In Taguchi method, the control factors were identified and optimized in a process and the orthogonal arrays (OA) were applied to manage a set of experiments. Results of these experiments were used to analyze the data and predict the quality of the produced components. Achievement of the desired results depends on a careful selection of process factors which could be divaricated into control and noise parameters. Selection of control factors must be made so that it can minimize the effect of noise factors [1,2].

The orthogonal array was used as a procedure in Taguchi method to study the all parameters with less number of experiments. Therefore, the Taguchi method recommends using the loss function to measure the proficiency characteristics.

The value of this loss function is assigned to signal-to-noise (S/N) ratio. There are three sets of the proficiency characteristics for analyzing the S/N ratio including (i) nominal-the-best, (ii) larger-the-better, (iii) smaller-the-better.

The steps of Taguchi method in an experimental design include (i) detection of the basic functions and their side effects, (ii) detection of the noise factors, investigation of the conditions and quality characteristics, (iii) detection of the target function to be optimized, (iv) detection of the control factors and their levels, (v) selection of an appropriate orthogonal array and the design of the Matrix, (vi) conducting Matrix experiment, (vii) testing data and predicting the optimum control factor levels and its proficiency and (viii) conducting the confirmation experiment [3].

A mixture of sulfuric and nitric acid is used in the process of toluene nitration for production of 2,4,6-trinitrotoluene (TNT) [4]. The different types of wastewaters of TNT production process namely "red water", "yellow water" and "pink water" hinge on the

*Corresponding author email: pouredal@gmail.com
Tel.: +98 31 4522 7382; Fax: +98 31 4522 5068

various steps of TNT production process. The addition of sodium sulfite to crude TNT yields a product with a dark "red" color, commonly known as "red water". Besides red water, other types of wastewater are also produced during the TNT manufacturing process. "Pink water" is the wastewater generated from water washing the purified TNT. Pink water contains up to 150 ppm TNT and other nitroaromatics, but little or no sulfonates. "Yellow-water" is produced when crude TNT is washed with water to remove excess nitric and sulfuric acids. Consequently, the yellow water not only consists of nitric and sulfuric acids, but also contains trace amounts of nitroaromatics [5,6].

The goal of advanced oxidation methods such as photodegradation process in presence of a semiconductor as photocatalyst is to generate active radicals including hydroxyl radical (HO^\bullet) and superoxide radical anion ($\text{O}_2^{\bullet-}$) to decompose pollutants [7,8]. TiO_2 semiconductor is a well known photocatalyst that is used in photodegradation process, for it has some advantages such as chemical stability, abundant, nontoxic, and cost-effective. Photogenerated holes in valence band of TiO_2 show the strong oxidizing power and thus the toxic organic compounds will be completely degraded to carbon dioxide while the photogenerated electrons in valence band are consumed by reducing oxygen (O_2). Therefore, titanium dioxide photocatalysts have the potential of an active photocatalyst for the purposes of air and water purification [9,10].

Among the advantages of TiO_2 photocatalyst, insensitivity of it to visible light is a restriction that is related to its band-gap of 3.0-3.2 eV [11,12]. The doping of transition metals and nonmetal impurities into the TiO_2 nanoparticles will improve the photocatalytic activity in visible region. Doping of N and Cu into TiO_2 is due to the optical response shift of active TiO_2 from the UV to the visible light [11-15]. That the doped N induced formation of localized occupied states in the absence of TiO_2 , brought about the visible light activity of N-doped samples. As consequence of the localized nature of the N-induced states, the hole generated by Vis-irradiation is less mobile than that generated by UV irradiation in the O 2p band and has also a lower direct oxidation potential for photocatalytic applications [10,11]. The metal ions such as Cu^{2+} can also serve as charge trapping sites, and thus decrease electron-hole recombination rate [13,14]. Moreover, the effect of doping on the activity depends on many factors including the method of doping, and thtype and concentration of dopant element [15-18].

In this research, the photocatalytic activity of doped TiO_2 nanoparticles by N and Cu was studied in the photodegradation process of yellow water of TNT production process. The sol-gel method was used for preparation of photocatalysts. The optimization of sample treatment process was improved using the Taguchi method as a statistical method. A model was proposed to indicate the relationship of dependent variables of photodegradation efficiency to independent variables. The verification of data and validation of predictor variables on the response variable were reported by statistical methods. The optimized photocatalyst was characterized by XRD, FE-SEM, EDS, BET and DRS methods.

2. Experimental

2.1. Synthesis of nanophotocatalysts

The nanoparticles of TiO_2 and doped TiO_2 with nitrogen and copper were prepared by the sol-gel method. The prepared nanoparticles were $\text{TiO}_2/\text{N}_{0.02}$, $\text{TiO}_2/\text{N}_{0.05}$, $\text{TiO}_2/\text{N}_{0.10}$, $\text{TiO}_2/\text{Cu}_{0.10}$ and $\text{TiO}_2/\text{Cu}_{0.05},\text{N}_{0.05}$. The amounts of doped elements were calculated as the weight percent in TiO_2 nanoparticles. The precursors were titanium isopropoxide, ammonium chloride and copper (II) nitrate. For synthesis of TiO_2 nanoparticles, 2.0 mL of titanium isopropoxide ($d=0.976 \text{ g}\cdot\text{cm}^{-3}$) was dissolved in 20 mL of anhydrous ethanol while quickly stirring for 30 min so that a homogeneous gel was formed [9,19]. Then, 10 mL of distilled water was added drop by drop to titanium sol. The pH of obtained mixture was controlled at $\text{pH} < 3$ by addition of acetic acid (1.0 mol L^{-1}) under stirring (120 min.) until a transparent solution was obtained. The prepared solution was aged at room temperature for 24 h for formation of stable suspension. The obtained solid was removed by filtration and then was heated at $70 \text{ }^\circ\text{C}$ for 2 h. The TiO_2 nanoparticles were calcined at $420 \text{ }^\circ\text{C}$ for 2 h in an oven. For preparation of other nanophotocatalysts, the calculated amounts of $\text{Cu}(\text{NO}_3)_2\cdot 3\text{H}_2\text{O}$ (1.3600 g in 10 mL ethanol for $\text{TiO}_2/\text{Cu}_{0.10}$) and NH_4Cl (0.0144, 0.0360 and 0.0720 g in 10 mL ethanol for $\text{TiO}_2/\text{N}_{0.02}$, $\text{TiO}_2/\text{N}_{0.05}$, $\text{TiO}_2/\text{N}_{0.10}$, respectively) were added to titanium solution. All chemicals were of highest purity from Merck Company.

2.2. Analysis of photocatalyst nanoparticles

The SEM images and EDS (energy dispersive spectroscopy) spectra of $\text{TiO}_2/\text{N}_{0.1}$ nanoparticles were obtained by a VEGA-Mira 3-XMU field emission - scanning electron microscope (FE-SEM). The XRD (X-ray diffraction) pattern of $\text{TiO}_2/\text{N}_{0.1}$ nanosized was

recorded by a Diffractometer Philips X. PERTPRO with anode of Cu ($\lambda=1.5406 \text{ \AA}$ of Cu K_{α}) and filter of Ni. The band gap of nanophotocatalysts was studied by diffuse reflectance UV/VIS spectra using a Perkin Elmer Lambda 35 spectrometer equipped with a Labsphere RSAPE-20 integration sphere with BaSO₄ as standard. The BET method and N₂ adsorption isotherms were used for estimation of nanoparticles surface. The nitrogen adsorption of gas at 77 K by a Belsorp Mini II instrument was used.

2.3. Photodegradation of yellow water samples

The wastewater of TNT production process as yellow water contains nitro-body compounds such as TNT, 3,5-dinitro-p-toluidine, 2,6-dinitrotoluene, 2,4-dinitrotoluene, 2,4-dinitrotoluene, 2-nitrotoluene, 4-nitrotoluene, 3-methyl-6-nitrobenzoic acid, 2-methyl-3,5-dinitrophenol, 5-methyl-2-nitrophenol, 3-methyl-2-nitrophenol and 1,3,5-trinitrobenzene [20]. The concentration of nitro-body compounds in a real sample of yellow water was determined by measuring of COD (chemical oxygen demand) of sample. The COD amount was obtained 3680 mg·L⁻¹ and density (d) of sample was 1.12 g·mL⁻¹. The real sample was prepared from a chemical industrial company of Isfahan province.

A homemade photocatalytic reactor with a light source of a 250 W halogen lamp was used for the photodegradation process. The distance between the lamp and the center of the cylindrical glass was 5 cm. A water-cooled jacket on the outside of its cell was used for controlling the temperature at 30 °C. The short wavelengths ($\lambda < 420 \text{ nm}$) of the light were cut off using a glass optical filter. The conditions of photodegradation process were as follows: volume of samples: 100 ml, dose of photocatalyst: 0.5-2.0 g·L⁻¹, irradiation time: 5-24 h. The real samples were diluted 250- 1000 times with distilled water. A period of 30 minutes in dark conditions was used for setting the adsorption/desorption equilibrium of pollutants on surface of photocatalysts. A magnetic stirrer was applied to make consistent the samples in duration of photodegradation process.

The absorbance of samples at wavelength of 350 nm before (A_o) and after (A_t) photodegradation process was employed for calculation of degradation efficiency (%D) in time of t. The %D was calculated using equation 1.

$$\%D = \frac{A_o - A_t}{A_o} \times 100$$

Eq. 1.

For example, the UV-Vis spectra of a sample containing 0.5 g·L⁻¹ of TiO₂/N_{0.02} nanophotocatalyst and diluted 250 times before and after the irradiation time of 5 h are shown in Fig. 1. As mentioned earlier, because the existence of several nitro aromatic compounds in a real sample of yellow water, the UV-Vis spectra is seen as wide spectra with maximum absorbance in 350 nm.

3. Results and Discussion

3.1. Results of Taguchi design

The identification of the effective factors of photodegradation process which affect the degradation efficiency is a significant step in experiments designs [2, 3]. Taguchi experimental design, an orthogonal array with four factors and four levels (L16), was selected, and experiments were conducted as per the standard orthogonal array [1]. The four important factors (Table 1) which mostly affect the degradation efficiency were: irradiation time, dose of photocatalyst, dilution times of the initial sample and the nature of photocatalyst [21,22]. The determination of limit of each control parameter was based on the preliminary experiments. In the first step, the selection of photocatalyst was the main scope of experimental design. The bare TiO₂, the TiO₂ doped with N and/or Cu and the TiO₂ doped with N and Cu were used.

The signal to noise ratio was calculated to determine the influence of each photodegradation process parameters on enhancing degradation efficiency of yellow water samples.

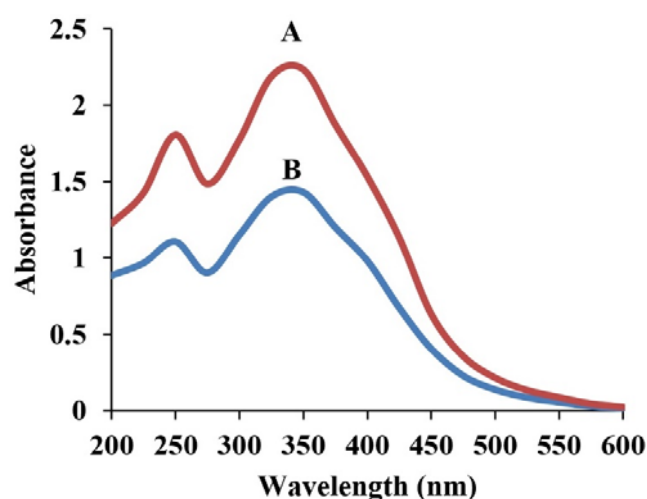


Fig. 1. UV-Vis spectra of a sample contain 0.5 g·L⁻¹ of TiO₂/N_{0.02} nanophotocatalyst, diluted 250 times before photodegradation (A) and after 5 h irradiation of (B).

Table 1. Control parameters and their levels for selection of the photocatalyst.

Control parameter	Level 1	Level 2	Level 3	Level 4
irradiation time (h)	6	12	18	24
dose of photocatalyst (g/L)	0.5	1.0	1.5	2.0
dilution times of sample	250	500	750	1000
nature of photocatalyst	TiO ₂	TiO ₂ /Cu _{0.10}	TiO ₂ /Cu _{0.05} ,N _{0.05}	TiO ₂ /N _{0.10}

The experimental results were converted into signal to noise (S/N) ratio values by equation 2 using Minitab 16 statistical software. The obtained results are detailed in the Table 2 and are shown in Fig. 2. In this study, the S/N ratio was chosen based on larger the better, in order to maximize the response of degradation efficiency [23].

$$S/N = -10 \log \left(\frac{1}{n} \sum_{i=1}^n \frac{1}{y_i^2} \right) \quad \text{Eq. 2.}$$

Where 'n' is the repetitions in each trial (n=4) and 'Y' is the experimental degradation efficiency. The higher S/N value of the response denotes the optimum parameters.

As can be seen from Table 2, the highest S/N ratios for experiment numbers of 9 and 15 were 38.8501 and 39.0170 respectively. The photocatalyst of TiO₂/N_{0.1}

showed the best result for degradation efficiency. In other words, the effect of N element versus Cu element and/or N and Cu elements as doped elements in TiO₂ nanoparticles is associated with higher photocatalytic activity. High photocatalytic activity is in agreement with results previously reported in the literature [11,12]. The advantages of nitrogen such as comparable atomic size, small ionization energy and stability are due to incentive for doping of nitrogen. Also, nitrogen doping is a modifier of the crystal structure of TiO₂ and suppress the recombination rate of photogenerated electrons and holes, which leads to enhanced photocatalytic activity compared to bare TiO₂ [10].

Also, the obtained results indicated the optimum conditions for dose of photocatalyst and dilution times of samples which are, respectively, 1.5 g·L⁻¹ and 750 times.

Table 2. The results and S/N ratios of experimental design for selection of photocatalyst.

Exp. No.	Irradiation time (h)	Dose of photocatalyst (g/L)	Dilution times of sample	Nature of photocatalyst	Degradation efficiency	S/N ratio
1	6	0.5	250	TiO ₂	21.0	26.4444
2	6	1.0	500	TiO ₂ /Cu	37.7	31.5268
3	6	1.5	750	TiO ₂ /Cu,N	51.5	34.2361
4	6	2.0	1000	TiO ₂ /N	55.4	34.8702
5	12	0.5	500	TiO ₂ /Cu,N	53.0	34.4855
6	12	1.0	250	TiO ₂ /N	62.2	35.8758
7	12	1.5	1000	TiO ₂	41.6	32.3819
8	12	2.0	750	TiO ₂ /Cu	48.0	33.6248
9	18	0.5	750	TiO ₂ /N	87.6	38.8501
10	18	1.0	1000	TiO ₂ /Cu,N	73.0	37.2665
11	18	1.5	250	TiO ₂ /Cu	58.8	35.3875
12	18	2.0	500	TiO ₂	44.4	32.9477
13	24	0.5	1000	TiO ₂ /Cu	59.4	35.4757
14	24	1.0	750	TiO ₂	47.4	33.5156
15	24	1.5	500	TiO ₂ /N	89.3	39.0170
16	24	2.0	250	TiO ₂ /Cu,N	80.8	38.1482

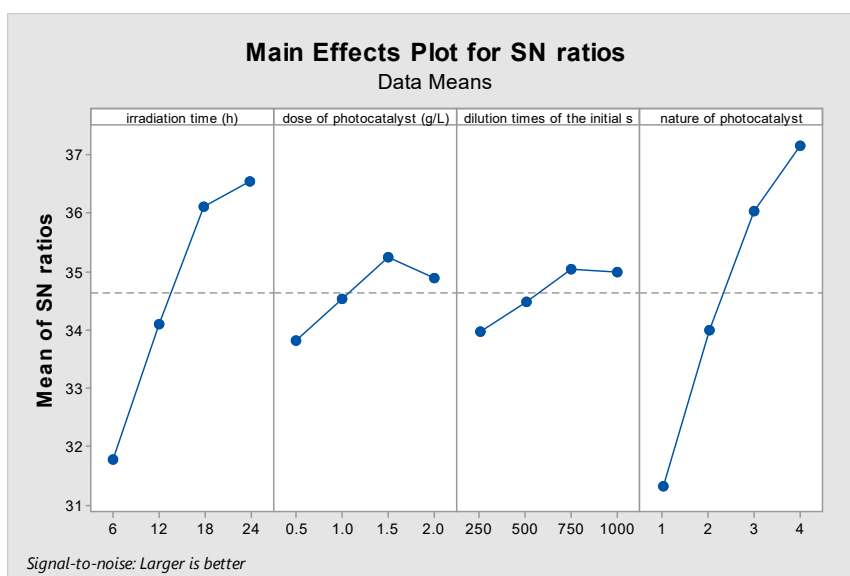


Fig. 2. Main effects plot for S/N ratio of degradation efficiency for experimental design of photocatalyst selection (nature of photocatalyst: 1; TiO₂, 2; TiO₂/Cu_{0.10}, 3; TiO₂/Cu_{0.05},N_{0.05}, 4; TiO₂/N_{0.1}) related to Tables 1 and 2.

As usual, the reduction of photodegradation process efficiency was seen in higher amounts of optimum photocatalyst dosage. This phenomenon is related to turbidity of samples and reduction efficiency of photocatalyst particles photoexcitation [24]. Supernumerary dilution of samples (> 750 times) also led to the reduction of treatment of yellow water sample because, the effective collision between the pollutant molecules and photocatalyst particles decreased. Also in high concentrations of pollutant samples, the degradation efficiency was reduced because of the photon absorption by the pollutant species [25]. However, the ranking of data based on S/N ratio in Table 3 has showed the order of importance of factors as follows: nature of photocatalyst > irradiation time > dose of photocatalyst > dilution times of sample.

The results of the first experimental design indicated that the TiO₂/N_{0.10} photocatalyst had the highest effect

on response of photodegradation process. Therefore, in the second step, the weight percent of N atoms in TiO₂ nanosized was optimized by the Taguchi experimental design. The four factors of irradiation time, dose of photocatalyst, the dilution times and weight (percent) of N doped in TiO₂ nanoparticles were used. The limit of control factors and the obtained results are summarized in Tables 4 and 5. The main effects plot for S/N ratio of degradation efficiency for optimization of %wt of N in TiO₂ nanoparticles is shown in Fig. 3. The ranking of data based on S/N ratio for the second Taguchi experimental design is given in Table 6.

The obtained results of the experimental design for optimization of %wt of N in TiO₂ nanoparticles revealed that the photocatalytic activity of TiO₂/N increased with addition of weight fraction of N. However, the maximum photocatalytic activity was seen for TiO₂/N_{0.1} nanoparticles.

Table 3. Response for signal to noise ratios for the experimental design of photocatalys selection.

Level	Irradiation time (h)	Dose of photocatalyst (g/L)	Dilution times of sample	Nature of photocatalyst
1	41.4	55.25	55.7	38.6
2	51.2	55.08	56.1	50.98
3	65.95	60.3	58.63	64.58
4	69.22	57.15	57.35	73.63
Delta	27.82	5.22	2.92	35.02
Rank	2	3	4	1

Table 4. Control parameters and their levels for optimization of %wt of N in TiO₂ nanoparticles.

Control parameter	Level 1	Level 2	Level 3	Level 4
Irradiation time (h)	5	10	15	20
Dose of photocatalyst (g/L)	0.5	1.0	1.5	2.0
Dilution times of sample	250	500	750	1000
%wt of N doped in TiO ₂ nanoparticles	2	5	10	12

Table 5. The results and S/N ratios of the experimental design for optimization of %wt of N in TiO₂ nanoparticles.

Exp. No.	Irradiation time (h)	Dose of photocatalyst (g/L)	Dilution times of sample	%wt of N doped in TiO ₂ nanoparticles	Degradation efficiency	S/N ratio
1	5	0.5	250	2	35.3	30.9555
2	5	1.0	500	5	55.9	34.9482
3	5	1.5	750	10	82.3	38.3080
4	5	2.0	1000	12	75.1	37.5128
5	10	0.5	500	10	68.6	36.7265
6	10	1.0	250	12	65.2	36.2850
7	10	1.5	1000	2	65.3	36.2983
8	10	2.0	750	5	62.4	35.9037
9	15	0.5	750	12	85.7	38.6596
10	15	1.0	1000	10	87.4	38.8302
11	15	1.5	250	5	70.1	36.9144
12	15	2.0	500	2	67.2	36.5474
13	20	0.5	1000	5	74.6	37.4548
14	20	1.0	750	2	70.9	37.0129
15	20	1.5	500	12	92.6	39.3322
16	20	2.0	250	10	91.4	39.2189

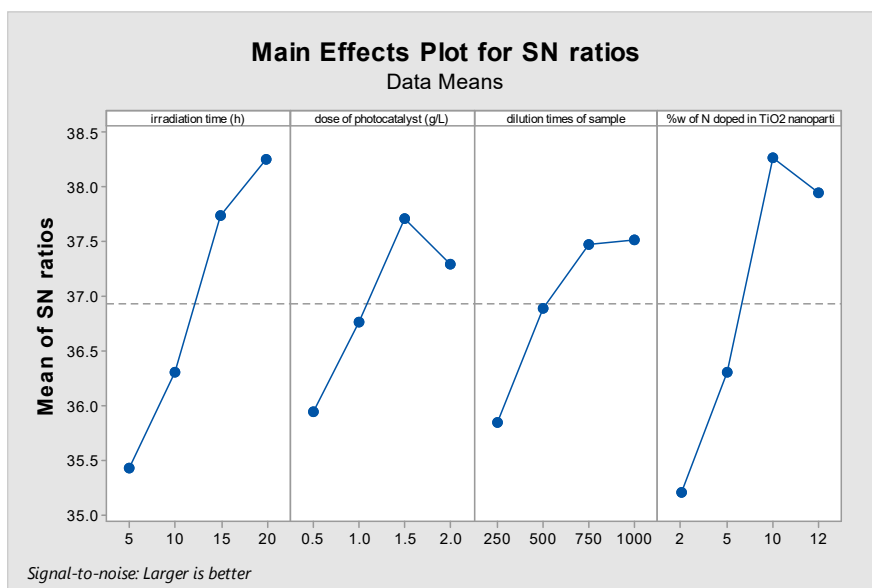


Fig. 3. Main effects plot for S/N ratio of degradation efficiency for optimization of %wt of N in TiO₂ nanoparticles related to Tables 4 and 5.

Table 6. Response for signal to noise ratios of experimental design for optimization of %wt of N in TiO₂ nanoparticles.

Level	Irradiation time (h)	Dose of photocatalyst (g/L)	Dilution times of sample	%wt of N doped in TiO ₂ nanoparticles
1	35.43	35.95	35.84	35.2
2	36.3	36.77	36.89	36.31
3	37.74	37.71	37.47	38.27
4	38.25	37.3	37.52	37.95
Delta	2.82	1.76	1.68	3.07
Rank	2	3	4	1

When the weight fraction of N was higher than the optimal value (10 %wt), the photocatalytic activity decreased. The increase of the doping amount of N (> 10 %wt) has less effect on the structure and size of modified TiO₂ [23]. Doping of nitrogen into TiO₂ photocatalyst increased the number of electrons that transferred from the valence band to the conduction band and enhanced the charge separation efficiency of the photoinduced electrons and holes. The electrons are trapped by the oxygen vacancy, while the holes are trapped by the doped nitrogen. On the other hand, the excited electron can transfer from the valence band to the new levels that exist higher than the conduction band introduced by nitrogen doping [26].

The variations of S/N ratio for other parameters which included: irradiation time, dose of photocatalyst and dilution times of sample were similar in both experimental designs (Fig. 2 and 3). The optimum amounts for photocatalyst dose and dilution times are 1.5 g·L⁻¹ and 750 times, respectively. Also, the ranking of parameters was similar in the results of both Tables 3 and 6. In other words, the importance of effective factors on the degradation efficiency was: the nature of photocatalyst > time of photodegradation > amount of photocatalyst > initial concentration of pollutants.

Multiple linear regression (MLR) method was applied to validate the relationship between dependent variable and the independent variables. The equation of MLR takes the following form.

$$Y = a + b_1 X_1 + b_2 X_2 + b_3 X_3 + \dots + b_k X_k \quad \text{Eq. 3.}$$

where Y is the dependent variable or response, X₁, X₂, X₃, ..., X_k are independent variables on predictors which the predictions are to be made and b₁, b₂, b₃, ..., b_k are the coefficients, the values of which were determined by the method of least squares. Multiple regression analysis was used to determine the relationship between dependent variable of degradation efficiency (Y) and parameters of irradiation time (X₁), dose of

photocatalyst (X₂), dilution times of sample (X₃) and %wt of N doped in TiO₂ nanoparticles (X₄). A linear equation (Eq. 4.) was obtained by the MLR analysis in Minitab-16.

$$Y = 20.492 + 1.461 X_1 + 6.330 X_2 + 0.014 X_3 + 2.291 X_4 \quad \text{Eq. 4.}$$

Therefore, the degradation efficiency can be predicted for operational factors in selected ranges. The regression coefficient (R²) is 0.887 which shows a fit to the experimental data. The P-values in the confidence level of 95% for independent variables were P < 0.05. Therefore, the null hypothesis is rejected and there is a meaningful relationship between the predictor's value and the response variable in the proposed model [27]. Contour plot of degradation versus %wt of N doped in TiO₂ nanoparticles, dilution times, dose of photocatalyst and irradiation time are shown in Fig. 4.

3.2. Analysis of TiO₂/N_{0.1} Photocatalyst

The results of Taguchi experimental design showed that for the yellow water sample in presence of TiO₂/N_{0.1} photocatalyst, the degradation is more than 90 percent. Therefore, this catalyst is characterized by the BET surface area analysis, diffuse reflectance UV/VIS spectra, X-ray diffraction pattern, EDS spectra and FE-SEM images.

The BET analysis indicates the surface area (150 m²·g⁻¹) of nanoparticles of TiO₂/N_{0.1}. The EDS spectra of TiO₂/N_{0.1} compound are shown in Fig. 5. The result of EDS analysis showed the percentage of N, O and Ti and confirmed the formation of N-TiO₂ doped nanoparticles. The Fig. 6 shows the FE-SEM images of nanoparticles of TiO₂/N_{0.1} in two scales of 500 and 200 nm. The formation of nanoparticles with approximately uniform distribution of size was confirmed by these images. The ordered particles for the prepared photocatalysts are also shown in FE-SEM images [28,29].

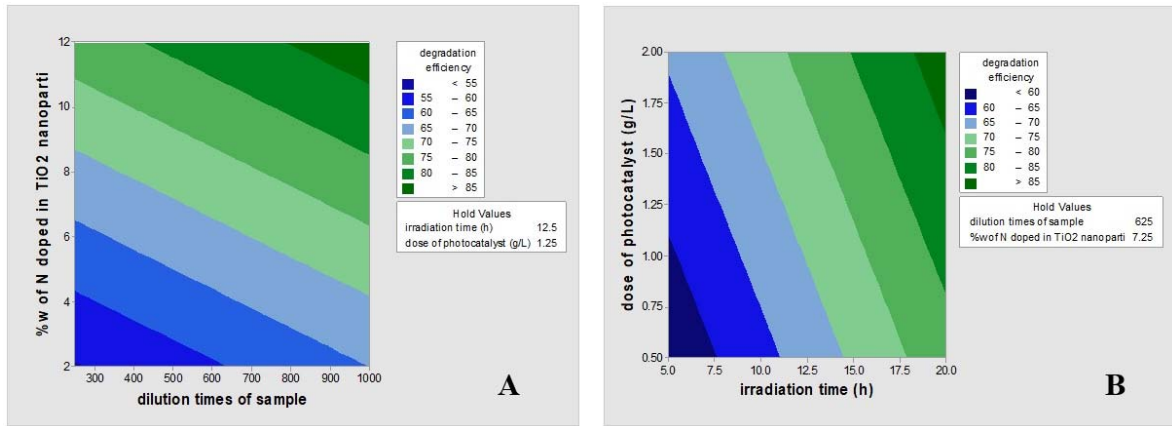


Fig. 4. Contour plot of (A) degradation vs. %wt of N doped in TiO₂ nanoparticles and dilution times, (B) degradation vs. dose of photocatalyst and irradiation time related to Tables 4 and 5.

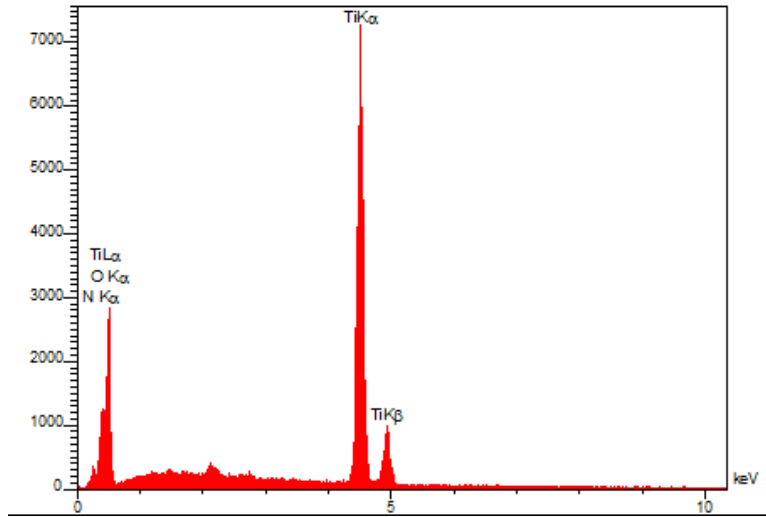


Fig. 5. The EDS spectrum of TiO₂/N_{0.1} nanoparticles.

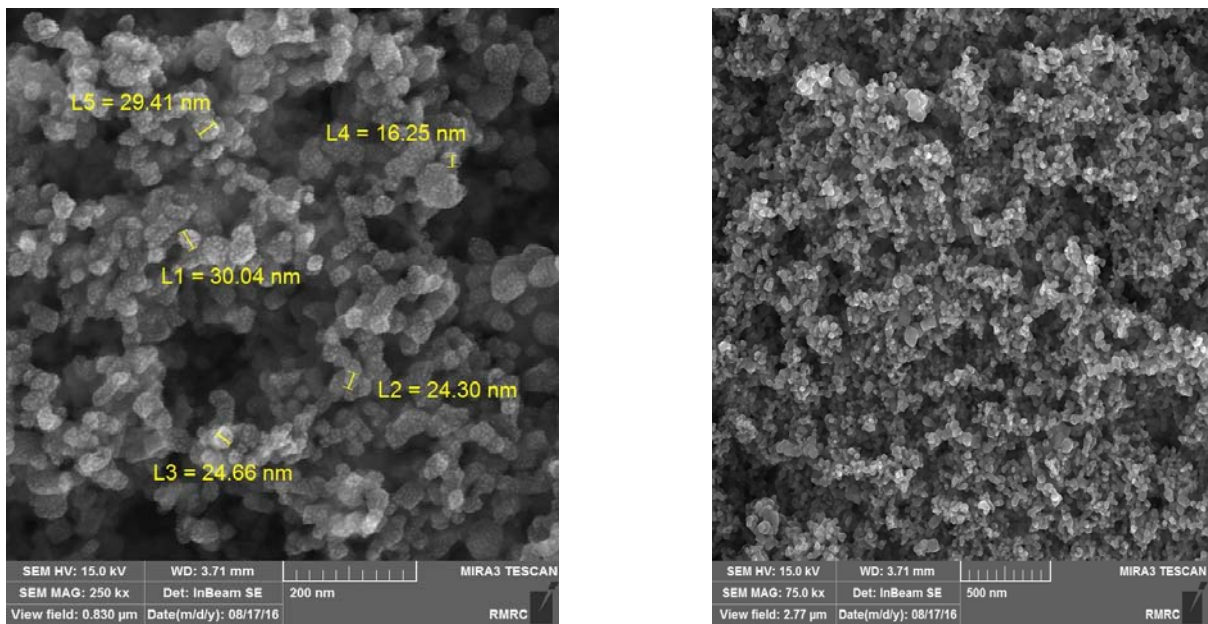


Fig. 6. The FE-SEM images of nanoparticles of TiO₂/N_{0.1} in two scales of 500 and 200 nm.

The XRD spectrum of TiO₂/N_{0.1} nanoparticles is shown in Fig. 7. The formation of anatase and rutile phases for prepared photocatalyst was proved by diffraction peaks at 2θ of 25, 38, 48, 54, 63, 69 and 75°. However, the anatase phase is superior to rutile phase [30,31]. The average size of TiO₂/N_{0.1} nanoparticles was also calculated using the Debye–Sherrer equation (Eq. 5.) [32]:

$$D = 0.89\lambda / \beta \cos\theta \quad \text{Eq. 5.}$$

where β is the width of the peak at half maximum, λ is the radiation wavelength, and θ is the Bragg angle [32]. The crystallite size for prepared nanoparticles was about 13.8 nm.

The absorbance spectra of TiO₂ and TiO₂/N_{0.1} nanoparticles in the domain of UV/Vis are indicated in Fig. 8. The wavelength (λ) of absorbance edge of 390 and 425 nm are reported for nanoparticles of TiO₂ and

TiO₂/N_{0.1}, respectively. Therefore, a red-shift of 35 nm occurred in doped TiO₂ with nitrogen [33]. The band-gap energies (E_g) of 3.17 and 2.92 eV were calculated by the equation of E_g (eV) = 1239.84 / λ (nm) for TiO₂ and TiO₂/N_{0.1} photocatalysts respectively. The λ value is wavelength of absorbance edge. Also, Fig. 9 shows the (αhv)^{1/2} versus E_{bg} (hv) for a direct band-gap transition using the Kubelca-Munc and Tauc plots, where α is the absorption coefficient and E_{bg} is the photon energy [34, 35]. The value of E_{bg} extrapolated to α = 0 gave an absorption energy, which corresponded to a band-gap energy. The values of 3.10 and 2.85 eV were obtained for TiO₂ and TiO₂/N_{0.1} nanoparticles, respectively (Fig. 9).

Augmenting activity of photocatalyst reduced band-gap energy by 0.25 eV. Increasing the number of electrons and holes of a semiconductor resulted from the reduction of band-gap energy of photocatalyst [36].

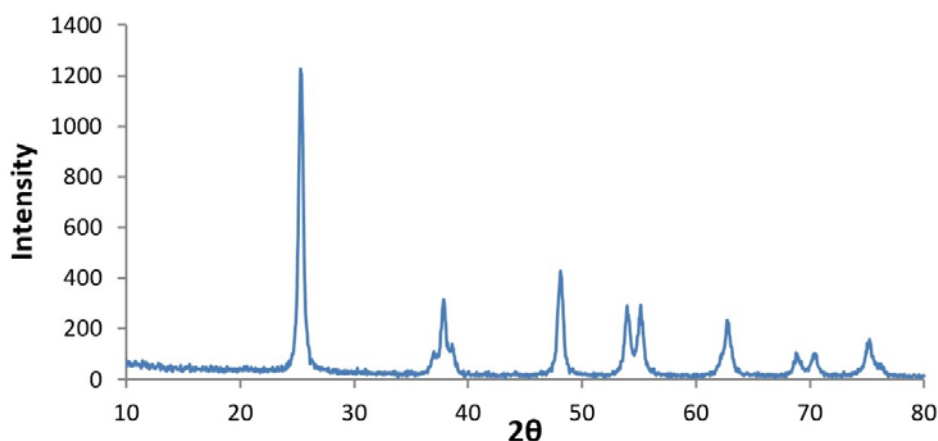


Fig. 7. The XRD spectrum of TiO₂/N_{0.1} nanoparticles.

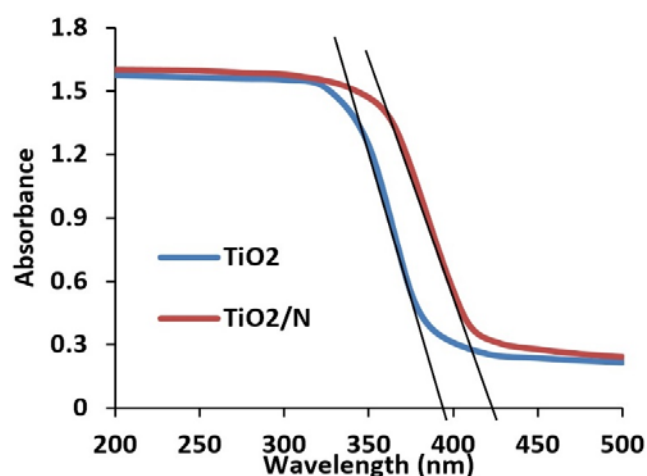


Fig. 8. The UV-Vis spectra of TiO₂ and TiO₂/N_{0.1} nanoparticles.

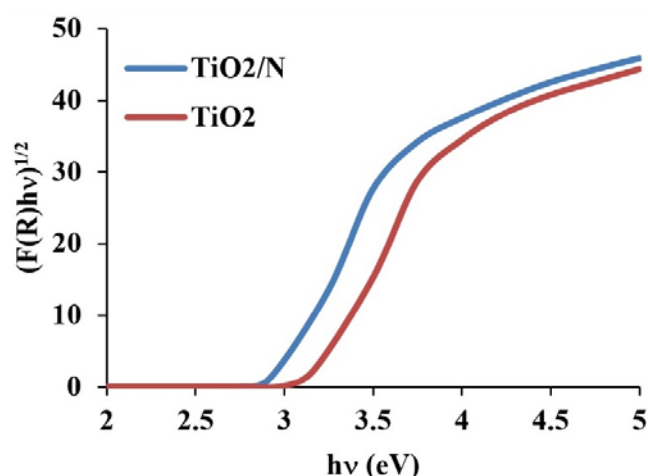


Fig. 9. The Tauc Plot (F(R)hv vs. hv) of TiO₂ and TiO₂/N_{0.1} nanoparticles.

4. Conclusions

Using of an experimental design technique such as Taguchi method can help to reduce the number of experiments for optimization of photodegradation process of wastewater sample. The Taguchi experimental design showed that the nitro-bodies compounds in the yellow water sample of TNT production were destructed more than 92% in optimized conditions. The controlled factors are optimized in doped TiO₂ nanoparticles with 10% wt. of nitrogen as photocatalyst, photocatalyst concentration of 1.5 g·L⁻¹ of, dilution times of 750 of preliminary sample and photodegradation time of 20 h.

The optimized photocatalyst of TiO₂/N_{0.1} presented the structure of anatase and rutile phases, nanoparticles size of less than 30 nm, band-gap energy of 2.92 eV and surface area of 150 m²·g⁻¹. The multiple linear regression (MLR) method indicated a meaningful relationship between the predictor's value and the response variable in the proposed model. The verification of photodegradation efficiency responses was confirmed by P-values of MLR technique data.

Acknowledgements

We would like to thank the research committee of Malek-ashtar University of Technology (MUT) for supporting this work.

References

- [1] G. Taguchi, S. Konishi, Taguchi methods, orthogonal arrays and linear graphs, tools for quality American supplier institute, American Supplier Institute (1987) p. 8-35.
- [2] D. Fratilia, C. Caizar, J. Cleaner Prod. 19 (2011) 640-645.
- [3] K. Raghukandan, K. Hokamoto, P. Manikandan, Met. Mater. Int. 10 (2004) 193-197.
- [4] M. Barreto-Rodrigues, F.T. Silva, T.C.B. Paiva, J. Hazard. Mater. 164 (2009) 385-388.
- [5] G. El Diwani, S. El Rafie, S. Hawash, Int. J. Environ. Sci. Tech. 6 (2009) 619-628.
- [6] J. Rodgers, N. Bunce, Water Res. 9 (2001) 2101-2111.
- [7] B. Khodadadi, Iran. J. Catal. 6 (2016) 305-311.
- [8] A. Besharati-Seidani, Iran. J. Catal. 6 (2016) 447-454.
- [9] H.R. Pouretedal, A.M. Sohrabi, J. Iran. Chem. Soc. 13 (2016) 73-79.
- [10] C. Di Valentin, E. Finazzi, G. Pacchioni, A. Selloni, S. Livraghi, M.C. Paganini, E. Giamello, Chem. Phys. 339 (2007) 44-56.
- [11] R. Asahi, T. Morikawa, H. Irie, T. Ohwaki, Chem. Rev. 114 (2014) 9824-9852.
- [12] T. Kaur, A. Pal Toor, R. Kumar Wanchoo, Int. J. Environ. Anal. Chem. 95 (2015) 494-507.
- [13] G. Colon, M. Maicu, M.C. Hidalgo, J.A. Navio, Appl. Catal. B 67 (2006) 41-51.
- [14] P. Pongwan, K. Wetchakun, S. Phanichphant, N. Wetchakun, Res. Chem. Intermed. 42 (2016) 2815-2830.
- [15] R. Jaiswal, J. Bharambe, N. Patel, Alpa Dashora, D.C. Kothari, A. Miotello, Appl. Catal. B 168 (2015) 333-341.
- [16] A. Nezamzadeh-Ejhieh, M. Bahrami, Desalin. Water Treat. 55 (2015) 1096-1104.
- [17] H. Zabihi-Mobarakeh, A. Nezamzadeh-Ejhieh, J. Ind. Eng. Chem. 26 (2015) 315-321.
- [18] H. Fallah Moafi, Iran. J. Catal. 6 (2016) 281-292.
- [19] H.R. Pouretedal, B. Afshari, Desalin. Water Treat. 57 (2016) 10941-10947.
- [20] F. Wei, Y. Zhang, F. Lv, P.K. Chu, Z. Ye, J. Hazard. Mater. 197 (2011) 352-360.
- [21] H.R. Pouretedal, S. Sabzevari, Desalin. Water Treat. 28 (2011) 247-254.
- [22] H.R. Pouretedala, M.H. Keshavarz, J. Alloys Compd. 501 (2010) 130-135.
- [23] S.S. Madaeni, S. Koocheki, Chem. Eng. J. 119 (2006) 37-44.
- [24] V. Mirkhani, S. Tangestaninejad, M. Moghadam, M.H. Habibi, A. Rostami Vartooni, J. Iran. Chem. Soc. 6 (2009) 800-807.
- [25] H.R. Pouretedal, O. Shevidi, M. Nasiri, F. Sotodeh Pourhasan, J. Iran. Chem. Soc. 13 (2016) 2267-2274.
- [26] Y. Cong, J. Zhang, F. Chen, M. Anpo, J. Phys. Chem. C 111 (2007) 6976-6982.
- [27] H.R. Pouretedal, M.H. Keshavarz, A. Abbasi, J. Iran. Chem. Soc. 12 (2015) 487-502.
- [28] S.M. El-Sheikh, T.M. Khedr, A. Hakki, A.A. Ismail, W.A. Badawy, D.W. Bahnemann, Sep. Purif. Technol. 173 (2017) 258-268.
- [29] E.M. Samsudin, S. Bee Abd Hamid, Appl. Surf. Sci. 391 (2017) 326-336.
- [30] Y. Zhang, K. Cheng, F. Lv, H. Huang, B. Fei, Y. He, Z. Ye, B. Shen, Colloids Surf. A 452 (2014) 103-108.
- [31] H.M. Yadav, J.S. Kim, S.H. Pawar, Korean J. Chem. Eng. 33 (2016) 1989-1998.
- [32] S. Aghdasi, M. Shokri, Iran. J. Catal. 6 (2016) 481-487.
- [33] S.J. Darzi, A.R. Mahjoub, S. Sarfi, Iran. J. Mater. Sci. Eng. 9 (202) 17-23.
- [34] H. Derikvandi, A. Nezamzadeh-Ejhieh, J. Hazard. Mater. 321 (2017) 629-638.
- [35] S. Azimi, A. Nezamzadeh-Ejhieh, J. Mol. Catal. A: Chem. 408 (2015) 152-160.
- [36] M.E. Olya, A. Pirkarami, Korean J. Chem. Eng. 32 (2015) 1586-1597.